The critical effects of matrices on cultured carcinoma cells: human tumor-derived matrix promotes cell invasive properties

Wafa Wahbi[1,2], Erika Naakka[1,2#], Katja Tuomainen[1,2#], Ilida Suleymanova[1,2], Annamari Arpalahti[1,2], Ilkka Miinalainen[3], Juho Vaananen[4], Reidar Grenman[5], Outi Monni[4], Ahmed Al-Samadi[1,2*&], Tuula Salo[1,2,6,7,8&]

1 Department of Oral and Maxillofacial Diseases, Clinicum, Faculty of Medicine, University of Helsinki, Helsinki, Finland

2 Translational Immunology Program, Faculty of Medicine, University of Helsinki

3 Biocenter Oulu Electron Microscopy Core Facility, University of Oulu, Oulu, Finland.

4 Applied Tumor Genomics Research Program, Faculty of Medicine, University of Helsinki, Helsinki, Finland 5 Department of Otolaryngology, Turku University, Turku, Finland.

6 Cancer and Translational Medicine Research Unit, University of Oulu, Oulu, Finland

7 Medical Research Centre, Oulu University Hospital, Oulu, Finland

8 Helsinki University Hospital, Helsinki, Finland

# Designates an equal contribution to this work.

& Supervised the work equally.

* Corresponding author: Ahmed Al-Samadi, Department of Oral and Maxillofacial Diseases, Clinicum, Biomedicum Helsinki 1, C223b P.O. Box 63 (Haartmaninkatu 8), 00014 University of Helsinki, Helsinki, Finland; E-mail: ahmed.al-samadi@helsinki.fi ; Tel: +358458947224.

Declaration of interests: The authors declare that they have no conflict of interest.

Abstract

The interaction between squamous cell carcinoma (SCC) cells and the tumor microenvironment (TME) plays a major role in cancer progression. Therefore, understanding the TME is essential for the development of cancer therapies.

We used four (primary and metastatic) head and neck (HN) SCC cell lines and cultured them on top of or within 5 matrices (mouse sarcoma-derived Matrigel®, rat collagen, human leiomyoma-derived Myogel, human fibronectin, and human fibrin). We performed several assays to study the effects of these matrices on the HNSCC behavior, such as proliferation, migration, and invasion, as well as cell morphology, and molecular gene profile.

Carcinoma cells exhibited different growth patterns depending on the matrix. While fibrin enhanced the proliferation of all the cell lines, collagen did not. The effects of the matrices on cancer cell migration were cell line dependent. Carcinoma cells in Myogel-collagen invaded faster in scratch wound invasion assay. On the other hand, in the spheroid invasion assay, three out of four cell lines invaded faster in Myogel-fibrin. These matrices significantly affected hundreds of genes and a number of pathways, but the effects were cell line dependent.

The matrix type played a major role in HNSCC cell phenotype. The effects of the ECMs were either constant, or cell line dependent. Based on these results, we suggest to select the most suitable matrix, which provides the closest condition to the *in vivo* TME, in order to get reliable results in *in vitro* experiments.

Keywords: Cancer, Extracellular Matrix, Invasion, Migration, Tumor Microenvironment.

Introduction

Squamous cell carcinoma cells are notably affected by their microenvironment that mainly includes extracellular matrix (ECM) and tumor stromal cells, such as cancer-associated fibroblasts (CAF), immune and endothelial cells (1). ECM is a major component of the TME and it is composed of a variety of proteins, proteoglycans, and polysaccharides (2). The structure and physical properties of tumor-associated ECM differ from normal tissue stroma (3). Changes in the ECM properties may cause variation in collagen deposition, promote the ECM stiffness, and upgrade cell survival and proliferation (4,5). ECM could also affect tumor stroma cells, such as CAFs, immune and endothelial cells (6). Therefore, understanding the SCC microenvironment is essential for the development of cancer therapies, which targets not only the cancer cells but also their environment that allows them to proliferate and spread.

In vitro, cancer cells are generally studied in 2D plastic wells. This usually leads to a loss of several important elements, which could affect the cell behavior and phenotype, making the 2D system not representative of the *in vivo* situation. In order to provide a more physiological environment for the cells, culture systems using different ECM mimicking three-dimensional matrices were introduced. Even though several matrices, which are extracted from different species such as mouse, rat, bovine, or prepared from non-animal material (7), were proposed to be used in 3D cell culture assays, selecting the most appropriate matrix for each cell type is not straightforward.

In spite of presence of several matrices from different origins, a human tumour-derived matrix is still missing from the market. Our group has invented the first tumour-derived matrix “Myogel” which is derived from leiomyoma tissue (8). Myogel has been used in several cancer *in vitro* studies (1,9-12). Myogel proteome differs greatly from the commonly used mouse sarcoma–derived Matrigel (8). We have shown recently that Myogel enhance the proliferation of freshly isolated cancer cells from primary tumor compared to plastic and Matrigel (10). Additionally, based on our recent publication, Myogel also improved the predictability of head and neck cancer drug testing (12). This setup, applying Myogel coated wells in drug testing, could reduce the number of failure clinical trials and reduce the cost of the anti-cancer drug development.

Here, we aimed to investigate the effects of several human- and animal-extracted ECMs, on the head and neck (HN) SCC cells. We used mouse tumor-derived Matrigel®, rat tail collagen, human plasma fibronectin, human-derived fibrin, and human tumor-derived Myogel; Bovine serum albumin (BSA) and uncoated wells were used as negative

controls. We selected four HNSCC cell lines as a model of SCC cells: UT-SCC-24 (tongue) and UT-SCC-42 (larynx), including primary (A) and corresponding metastasis (B). We compared the effects of these matrices with the non-coated plastic analyzing cell morphology, proliferation, migration, and invasion. We also studied the effects of these matrices on the molecular profile of these cells using transcriptome profiling.

Materials and Methods

Cell lines

UT-SCC cell line series, UT-SCC-24A (Primary tongue cancer, RRID:CVCL_7826), UT-SCC-24B (Metastatic tongue cancer, RRID:CVCL_7827) and UT-SCC-42 (larynx), including primary (A, RRID:CVCL_7847) and metastatic (B, RRID:CVCL_7848). Were kindly provided by Prof. Grenman (Department of Otolaryngology, Turku University, Turku, Finland). UT-SCC cells were grown in DMEM-F12 medium (Gibco™/Invitrogen, Tokyo, Japan) supplemented with 10% foetal bovine serum, 1% penicillin/streptomycin and 250µg/mL amphotericin B (all from Sigma-Aldrich, St. Louis, Mo, USA). All the cell lines were cultured in a humidified incubator (37°C, 5% CO2, 95% humidity, Binder, Tuttlingen, Germany).

Locally established four cell lines were isolated from two HNSCC patients, having both primary and metastatic tumors. Details of the cell lines are provided in supplementary Table 1.

Preparation of the wells and light microscope imaging of cells morphology

Ninety-six-well plates with black well walls and clear bottoms (Essen Bioscience, Ann Arbor, MI, USA) were used for coating. The plate was placed on ice and 50 µL/well of 0.5 mg/mL Matrigel and collagen (Corning, Corning, NY, USA) were dispensed using cold pipet tips. The plate was placed in the incubator for 30 minutes, then 50 µL/well of 0.01mg/mL BSA (Sigma-Aldrich), 0.01 mg/mL fibronectin (Sigma-Aldrich), 0.5 mg/mL Myogel (Lab made, see below)

and 0.5mg/mL fibrin (For fibrin preparation, see below) was added to the plate. The plate was incubated at the cell culture incubator for overnight. Cells were detached from flasks using trypsin-EDTA and seeded at the density of 1000 cells/well in 100 µL of complete medium.

Myogel was prepared from human uterus leiomyoma tissue following the instructions in Salo et al., 2015 (8). Briefly, tissue pieces were frozen using liquid nitrogen and crushed into a powder with CryoMill (Retsch, Haan, Germany). A volume of 20 ml of ice cold NaCl buffer (3.4 M, pH 7.4) was mixed with 10 g of tissue powder and centrifuged. 20 ml of the same NaCl buffer was used to homogenize the pellet with a T18 Ultra-Turrax (IKA®-Werke GmbH & Co. KG, Staufen, Germany). DC Protein Assay (Bio-Rad, Hercules, California, United States) was used to measure the protein concentration in each preparation. The Myogel solution was stored in small (≤1 ml) aliquots at −20 °C.

Fibrin was prepared using 0.5 mg/mL fibrinogen (Merck, Darmstadt, Germany), 33,3 µg/mL aprotinin (Sigma-Aldrich) and 0,34 U/mL thrombin (Sigma-Aldrich).

To observe the effect of matrices on cell morphology, pictures of each well were taken after 3 days using the reverse Nikon Digital sight DS-U3 microscope (Nikon, Tokyo, Japan) at x10 and x20 magnification.

Scanning electron microscope assay

We used two cell lines (UT-SCC-42A and UT-SCC-42B) to study the cell-matrix interaction under scanning electron microscope. Glass coverslips were inserted into wells of a 24 well plate (Corning) and coated using 300 µL of coating suspension (using the same concentrations as above for each matrix). Six thousand cells were seeded on each coverslip and incubated for 2 days. For fixation,

we performed several washing steps with 500 µL of phosphate-buffered saline (PBS), and then we added 500 µL of 4% formaldehyde and kept it for 20 minutes at room temperature. After that, we washed the wells with PBS again for 3 times, 5 minutes each. Samples were dehydrated using graded ethanol series and dried using K850 critical point dryer (Quorum Technologies, UK). After drying, samples were attached to aluminium stubs with double-sided carbon tape and coated with 5 nm of platinum using Q150T ES sputter coater (Quorum Technologies, UK). Samples were imaged with Sigma HD-VP field-emission scanning electron microscope (Carl Zeiss, Oberkochen, Germany).

Proliferation luminescent cell viability assay

For proliferation, we used the same experiment settings as in the imaging assay. After 3 days, the plate was taken out from the incubator to room temperature for 15 min before starting the assay. 100 µL of CellTiter-Glo was dispensed in each well. The plate was put on a plate shaker (Heidolph, Schwabach, Germany) for 5 min at 450 rpm and then in plate spinner (Thermo Scientific, Massachusetts, USA) for 5 min at 1000 rpm. Finally, the plate was placed in the BMG PHERAstar FS (BMG Labtech, Offenburg, Germany) plate reader to detect cell viability.

Scratch wound cell migration assay

The same coating protocol was used as before, except that the gels were sucked out before seeding the cells. We seeded the cells at the following density: 25000/well for UT-SCC-24A and UT-SCC-42B and 30000/well for UT-SCC-24B and UT-SCC-42A. Matrigel was not used in this experiment as the cells were forming clusters on top of the Matrigel leading to difficulties in getting a smooth scratch. The wound maker (Essen Bioscience) was used to achieve homogeneous scratch wounds.

Wounds were checked under the light microscope and the media was changed for all the wells. The plate was placed in IncuCyte ZOOM incubator (Essen Bioscience), and wounds confluences were monitored using the IncuCyte Live-Cell Imaging System (Essen Bioscience). Images were taken each hour for 20 hours. Supplementary Video (Online Resource 1) shows the migration of the UT-SCC-42A cells on top of Myogel.

Scratch wound cell invasion assay

Four gels were used in this experiment: collagen, Myogel-collagen, fibrin, and Myogel-fibrin at the concentration of 1 mg/mL for all of them, as instructed by the manufacturer (Essen Bioscience). Similar to the migration experiment, wells were coated, cells were seeded and a scratch wound was made. After that, 50 µL of the gels were added. Once the gels solidified, 50 µL of media was added. The plate was placed in IncuCyte ZOOM incubator, and wounds confluences were monitored using the IncuCyte Live-Cell Imaging System (Essen Bioscience). Images were taken each hour for 48 hours. Supplementary Video (Online Resource 2) shows the invasion of the UT-SCC-42A within Myogel-collagen.

Spheroid Invasion Assay

Cells were seeded at the concentration of 1000 cells/well in 50 µL using ultra-low attachment 96-well round bottom plate wells (Corning). The plate was incubated for 4 days to allow spheroid formation. Spheroids were embedded in 100 µL of Matrigel (0.5 mg/mL), collagen (0.5 mg/mL), Myogel-collagen (0.5 mg/mL), fibrin (0.5 mg/mL fibrinogen + 0.3 U/mL Thrombin + 3.33 mg/mL Aprotinin), and Myogel-fibrin (0.5 mg/mL). Gels were allowed to solidify for 30 minutes and then 100 µL of DMEM was added into each well. The plate was incubated for 4 days and pictures were taken every day using Nikon Digital sight DS-U3 microscope (Nikon) at x4 magnification. The used protocol is explained in detail in Naakka et al., 2019 (9)–. We analyzed the area covered by cells using ilastik and ImageJ (Wayne Rasband, National Institute of Mental Health, Bethesda, MD, USA). Once ilastik detected area covered by cells, we used a custom plugin, written for ImageJ, to measure the area. The plugin converts the image to black and white image. All pixels outside the area are set to zero, the cells area is set to one. The total area is measured as a number of pixels equal to one.

Microarray

UT-SCC-24A and UT-SCC-24B cell lines were used to study the effects of different matrices on the molecular gene profile using RNA sequencing transcriptome profiles. Wells of 24 well-plates were coated with 150 µL of gels (using the same concentrations as in the imaging assay) and seeded with 150 000 cells. Cells were left on the gels for 24 hours and lysed using RLT buffer. RNA was

extracted using RNeasy Kit (Qiagen, Düsseldorf, Germany) according to manufacturer instructions. In case some clots or fragments of gels existed in the cell lysate, sonication was used to solubilize them. The quality of total RNA was assessed with a TapeStation (Agilent Technologies, Santa Clara, CA, USA), and only samples of high quality (RNA integrity value >8) were included in the analyses. The starting amount of total RNA was 100 ng. The labeling and hybridization were done according to the manufacturer's instructions by using Applied Biosystems GeneChipTM WT PLUS Reagent Kit and Manual Target Preparation for GeneChipTM Whole Transcript (WT) Expression Arrays (UserGuide 23 January 2017; Thermo Fisher Scientific). Fifteen micrograms of cRNA were used for single-stranded cDNA-synthesis (sscDNA) and a total of 5,5 ug of sscDNA was fragmented. A total of 2.3 µg was hybridized on Clariom S Affymetrix array.

Gene set enrichment and pathway analysis

Gene set enrichment analysis (GSEA, http://software.broadinstitute.org/gsea/index.jsp) (13) was carried out to connect gene expression signatures with previously known gene sets and pathways. The analysis was performed for each cell line and matrix combination separately using the full expression data set against C2: curated gene sets available at broad institute web page. Genes were ranked using signal-to-noise ratio and gene set permutation was used for FDR estimation and enrichment score adjustment. Additional analyses for Gene Ontology enrichment and KEGG pathway visualization were carried out in R (v. 3.5.3) using packages gage (generally applicable gene set enrichment, v. 2.32.1) (14) and pathview (v. 1.22.3) (15). Both the GSEA and additional R analyses were performed by the Functional Genomics Unit (FuGU) at the University of Helsinki. Two samples (UT-SCC-24A/fibrin and UT-SCC-24B/fibrin) were excluded from the analysis as a result of probability of mislabelling.

Analysis of cells circularity and their surface area

Cells circularity and surface area were measured using ImageJ software (Wayne Rasband, National Institute of Mental Health, Bethesda, MD, USA). The experiments were done four times independently. Two wells were used for each condition and 3 cells were randomly selected and measured from each well.

Statistical analysis

All experiments were repeated independently at least three times, each in duplicate or triplicate. Values are given as means ± standard deviations. All statistical analyses were performed using SPSS (IBM SPSS Statistics for Windows, version 21.0; Armonk NY, IBM Corp.) To determine the statistical significance, we performed one-way analysis of variance (ANOVA) followed by Bonferroni correction. We set statistical significance to $p<0.05$. P values were presented as follows: * = $P \leq 0.05$, ** = $P \leq 0.01$, *** = $P \leq 0.001$, **** = $P \leq 0.0001$. Origin lab software was used to create the figures.

Results:

SCC cell~~s~~ morphology is affected by the matrix type

Cancer cell morphology was affected by the type of matrix (Figure 1). While cells seeded on BSA had similar morphology to the cells in the control wells, cells on Matrigel formed round clusters. Cells on fibronectin had a more flattened surface than cells on the other matrices. Cells on Myogel, fibrin, and collagen were more spindle in shape and there were fibers surrounding the cells. Here we present the pictures of UT-SCC-24B cells only since the other cell lines behaved similarly (data not shown).

For all the cell lines, cells on Matrigel had the ~~tendency of~~ highest circularity value (above 0.8 out of 1) due to the formation of cell clusters, though circularity was close to 0.8 in many instances with the other matrices as well (Figure 2). ~~The other matrices did not have any clear effect on cell circularity.~~

The majority of the cell lines, except UT-SCC-24A, seeded on top of fibronectin had higher surface area than in the other conditions, but this difference did not reach statistical significance (Figure 3). UT-SCC-24A cultured on top of fibrin had significantly lower surface area compared to the cells on plastic wells (Figure 3).

Cell~~s~~-matrix interaction

Scanning electron microscope was used to observe the differences between structures of matrices (Figure 4). While Matrigel has a fiber sheet structure, Myogel's structure was in form of thin

unorganized fibers together with small globular proteins. Fibrin has abundant thin fibers. Collagen presented helical fibers structure. Fibronectin did not show a fibril structure.

The SEM pictures revealed the interaction between the cells and the matrices (Figure 5). Cells cultured on BSA behaved similarly to the controls. On top of Matrigel, cells formed small clusters. Cells on fibronectin tend to be flat with large surface areas. As for Myogel, cells were gathered in groups and they were in contact with several fibers. For fibrin and collagen, cells were embedded within the matrix fibers.

Fibrin increased and collagen reduced SCC proliferation, while matrix effect on cell migration was cell line dependent.

The proliferation rate for all the tested cell lines was the highest on top of fibrin, and the lowest on top of collagen (Figure 6). This difference was significant for the fibrin-coated wells in case of UT-SCC-24A, 24B, and 42A, and for the collagen-coated wells in case of UT-SCC-24A and 42A.

The scratch wound cell migration assay showed that some matrices were able to affect cancer cell migration but this effect was cell line-dependent (Figure 7). Opposite to the proliferation results, collagen -induced UT-SCC-24B migration and fibrin reduced it. For UT-SCC-42A, cells cultured on top of Myogel were migrating significantly slower compared to the control. Matrigel was not used for migration assay since the cells formed clusters and a homogeneous wound was not possible to be achieved.

Myogel induced SCC cell invasion

Cancer cells had different invasion speeds in the scratch wound invasion assay based on the matrix used (Figure 8). Cells cultured within Myogel-collagen invaded the fastest. On the other hand, cells did not invade through Myogel-fibrin and fibrin matrices. Myogel was able to induce cancer cells~~s~~ invasion when added to the collagen~~,~~ significantly in case of UT-SCC-42 A and B.

Figure 10). Myogel was able to significantly induce cancer cell invasion when added to the fibrin in case of UT-SCC-24B and 42A (Figure 10).

Fibrin had the highest and BSA and fibronectin the lowest impact on SCC cell molecular profile

In order to understand the mechanism behind the effect of different matrices on the SCC cells behavior, we studied the molecular gene profile using RNA sequencing transcriptome profiles. Matrices were able to change the gene expression of hundreds of genes (Supplementary Table 2). While cells seeded on fibrin had the largest difference (574 and 103 genes significantly affected, $P \leq 0.05$, in UTSCC-24A and B, respectively), cells on BSA (15 and 19 genes significantly affected in UTSCC-24A and B, respectively) and fibronectin (9 and 15 genes significantly affected in UTSCC-24A and B, respectively) showed the least difference in their genes expression compared with the cells cultured on plastic (Supplementary Table 2). The most significantly affected genes for each matrix are presented in Supplementary Table 3.

Gene ontology enrichment analysis revealed several affected ontology groups (Supplementary Table 4). These were both matrix and cell line dependent. The 10 most up- and downregulated biological processes indicated by analysis are presented in Supplementary Table 5.

Due to the large variation between the two cell lines, we unfortunately were not able to detect specific genes or ontology groups directly responsible for the changes in the SCC cells behavior.

Discussion

ECMs are increasingly used in cancer research to study different aspects of cancer cell behavior, such as proliferation, migration, invasion and drug testing. The usage of these matrices was regarded as a leap in moving ~~towards~~ closer to *in vivo* conditions than the traditional 2D cell culture on plastic. This is mainly due to the ability of these matrices to provide essential elements needed for the cell-cell and cell-matrix interaction. Due to the presence of several types of ECM, such as Matrigel, Myogel, collagen, and fibrin, choosing the most suitable matrix that fits with the needed assays without knowing its properties and effects could be risking the reliability of the results ~~is difficult~~. Unfortunately, several researchers select the matrix type for their assay based only on the availability, cost, and easiness of the matrix handling, without paying attention to the effect~~s~~ of the matrix on ~~the~~ cancer cell~~s~~ behavior. Using a non-representative tumor matrix could lead to non-reliable results. In this project, we pointed out the significant differences in SCC cells behavior and their gene profile when tested with various matrices. This emphasizes the importance of selecting the most suitable matrix for each assay.

We first studied the effect of ~~six~~ five matrices on the HNSCC cell morphology. Interestingly, all the used cell lines formed cell round clusters when cultured on top of Matrigel, which is the most common commercial extracellular matrix used in *in vitro* experiments. Our results are in line with several other studies showing similar cell behavior on Matrigel in different cancer types ~~–~~(16-18). Forming cell clusters may be due to the presence of a large amount of basement membrane proteins in Matrigel which seems to hold the cells together (19). Even though mimicking the basement membrane is considered as an advantage for Matrigel, this feature is a disadvantage in invasion assays due to the difficulties of cancer cells to invade through it. Opposite to the Matrigel, cells cultured on top of Myogel, fibrin and collagen had a spindle shape, which represents more the invasive phenotype of carcinoma cells, as reported in several publications (16,20,21). This morphology may represent an epithelial-mesenchymal transition (EMT), which is an important feature for cancer cell migration and invasion (22-24). Cells cultured on fibronectin had a unique flattened shape with a large surface area. This shape could be explained by the presence of the

347 $\alpha_5\beta_1$ integrin (25) which is a fibronectin receptor (26), leading to an interaction that requires
348 traction forces provided by the matrix.
349 To confirm our visual observation of cell morphology, we measured the circularity and surface
350 area of the cells. As expected, cells cultured on top of Matrigel had the highest circularity value
351 due to the formation of round clusters. On the other hand, cells cultured on fibronectin had the
352 highest surface area due to the flat shape of the cells.
353 In order to get a better understanding of the cell-matrix interaction, we visualized the cells and the
354 matrix under scanning electron microscope. As expected, most of the used matrices, except BSA
355 and fibronectin, have fibril structures. The fibril structure of the matrices differed from one matrix
356 to another in the terms of the amount of the fibers (rich *vs* poor) and thickness of the fibers (thick
357 *vs* thin). All these differences, in addition to the presence or absence of several growth factors and
358 other proteins, explain the differences in the behavior of cancer cells from one matrix to another.
359 The interaction between the cells and the matrix was also different from one matrix to another.
360 For some matrices, as in Myogel, the cells were surrounded by fibers, while for others, cells were
361 either on top of the matrix (Matrigel) or embedded in it (fibrin and collagen).
362 As cell viability assay is one of the main assays used in *in vitro* cancer research, we studied if the
363 matrix itself could have an effect on cancer cell proliferation. Interestingly, one pattern was found
364 in all the tested cell lines with the highest proliferation rate detected in the fibrin-coated wells and
365 the lowest in the collagen wells. Our results are in line with Simpson-Haidaris *et al*. who reported
366 similar results for breast cancer cells MCF-7 cultured on fibrin (27). On the other hand, our results
367 are opposite to Chen *et al*., who reported a higher proliferation rate of MCF-7 cells when cultured
368 on a porous collagen scaffold (28), suggesting that the effect of the collagen matrix is cell line
369 dependent. Other matrices did not have a significant effect on HNSCC cell proliferation which goes
370 hand by hand with some studies (29,30).
371 Next, we studied the effect of the different matrices on cancer cell migration. Our results
372 revealed that the effects of the studied matrices on HNSCC migration were cell line dependent,
373 and the significant effects were assured by collagen, Myogel, and fibrin for some cell lines. It
374 was an interest to us to notice the opposite effect of collagen and fibrin matrices on the
375 proliferation and migration behavior of the UT-SCC-24B cell line. While these cells had the
376 highest rate of proliferation on fibrin and the lowest on collagen, the opposite happened in cell

migration. This may return to the fact that the low proliferative cancer cells have high migration capacity and *vice versa* (31).

Our scratch wound cell invasion assay showed that cells cultured within Myogel-collagen 3D matrix invaded faster than cells within other matrices. This induction of invasion was mainly due to Myogel since we also cultured HNSSC cells within collagen alone and the invasion speed was lower. A similar effect of Myogel was observed on other cell lines (1). Cancer cells did not invade through fibrin or Myogel-fibrin, which ~~might return~~may be due to the fibrin's compact structure.

Similar to scratch wound cell invasion assay, Myogel was able to induce invasion in spheroids. However, in scratch wound assay, Myogel-collagen was the most invasive inductive matrix in all 4 cell lines, while in spheroid 3 out of 4 cell lines invaded ~~the~~ fastest in Myogel-fibrin and one in Myogel-collagen. This difference is most likely due to differences in the concentration of the gels in the two assays (1 mg/ml in the scratch wound invasion and 0.5 mg/ml in the spheroid invasion assays). Gels concentration were choosen either following the manufacturer instruction (scratch wound invasion assay) or after lab optimization (spherioid invasion assay). Based on both invasion assays, adding Myogel seems to improve the speed of HNSCC cancer cell~~s~~ invasion. This Myogel property could help in studying low invasive cancer cell lines and testing anti-invasive cancer treatments.

Matrigel has been the mostly used matrix for *in vitro* 3D cancer research. However, it should be kept in mind that it is derived from mouse sarcoma containing mostly basement membrane proteins (19)~~.~~. Due to its nature, in our invasion assays, cells failed to invade efficiently.

Based on our mRNA microarray results, the matrix type was able to significantly affect hundreds of genes and several pathways. Interestingly, these genes and pathways were not shared between matrices or cell lines but were matrix and cell line dependent. This was the reason that unfortunately we were not able to detect specific gene or pathway responsible for the changes in the SCC cells behavior. These results indicate that one cell line cannot represent the behavior of any studied tumor type, and always more than one cell line should be used in *in vitro* experiments.

Our study revealed important effects of the ECMs on HNSCC cells' behavior, morphology, and molecular gene profile. We showed here that the ECMs are not idle elements, but instead, they have significant effects on the *in vitro* results. We believe that for each assay, selecting the

appropriate matrix, based on its characteristics and the studied cell line, is necessary to get reliable results in *in vitro* experiments. In theory, selecting human tumor-derived matrix could represent the closest condition to the *in vivo* tumor microenvironment which increases the reliability of the *in vitro* cancer cells testing.

Acknowledgment:

We acknowledge the funders of this study: the Sigrid Jusélius Foundation, The Cancer Society of Finland, Oulu University Hospital MRC grant, the Emil Aaltonen Foundation, Helsinki University Central Hospital Research Funds, and Jane and Aatos Erkkos Foundation.

References:

(1) Salo T, Dourado MR, Sundquist E, Apu EH, Alahuhta I, Tuomainen K, et al. Organotypic three-dimensional assays based on human leiomyoma–derived matrices. Philosophical Transactions of the Royal Society B: Biological Sciences 2018;373(1737):20160482.

(2) Whittaker CA, Bergeron K, Whittle J, Brandhorst BP, Burke RD, Hynes RO. The echinoderm adhesome. Developmental Biology 2006;300(1):252-266.

(3) Provenzano PP, Eliceiri KW, Campbell JM, Inman DR, White JG, Keely PJ. Collagen reorganization at the tumor-stromal interface facilitates local invasion. BMC Medicine 2006;4(1):38.

(4) Sundquist E, Renko O, Salo S, Magga J, Cervigne NK, Nyberg P, et al. Neoplastic extracellular matrix environment promotes cancer invasion in vitro. Experimental cell research 2016;344(2):229-240.

(5) Lu P, Weaver VM, Werb Z. The extracellular matrix: A dynamic niche in cancer progression. Journal of Cell Biology 2012;196(4):395-406.

(6) Quante M, Tu SP, Tomita H, Gonda T, Wang SSW, Takashi S, et al. Bone Marrow-Derived Myofibroblasts Contribute to the Mesenchymal Stem Cell Niche and Promote Tumor Growth. Cancer Cell 2011;19(2):257-272.

(7) Lou Y, Kanninen L, Kuisma T, Niklander J, Noon LA, Burks D, et al. The Use of Nanofibrillar Cellulose Hydrogel As a Flexible Three-Dimensional Model to Culture Human Pluripotent Stem Cells. Stem Cells and Development 2014;23(4):380-392.

(8) Salo T, Sutinen M, Hoque Apu E, Sundquist E, Cervigne NK, de Oliveira CE, et al. A novel human leiomyoma tissue derived matrix for cell culture studies. BMC Cancer 2015;15(1):981.

(9) Naakka E, Tuomainen K, Wistrand H, Palkama M, Suleymanova I, Al-Samadi A, et al. Fully Human Tumor-based Matrix in Three-dimensional Spheroid Invasion Assay. Journal of Visualized Experiments 2019(147):e59567.

(10) Al-Samadi A, Poor B, Tuomainen K, Liu V, Hyytiäinen A, Suleymanova I, et al. In vitro humanized 3D microfluidic chip for testing personalized immunotherapeutics for head and neck cancer patients. Experimental Cell Research 2019;383(2):111508.

(11) Almahmoudi R, Salem A, Murshid S, Dourado RM, Apu HE, Salo T, et al. Interleukin-17F Has Anti-Tumor Effects in Oral Tongue Cancer. Cancers 2019;11(5).

(12) Tuomainen K, Al-Samadi A, Potdar S, Turunen L, Turunen M, Karhemo P, et al. Human Tumor–Derived Matrix Improves the Predictability of Head and Neck Cancer Drug Testing. Cancers 2019;12(1).

(13) Subramanian A, Tamayo P, Mootha VK, Mukherjee S, Ebert BL, Gillette MA, et al. Gene set enrichment analysis: A knowledge-based approach for interpreting genome-wide expression profiles. Proceedings of the National Academy of Sciences USA 2005;102(43):15545.

(14) Luo W, Friedman MS, Shedden K, Hankenson KD, Woolf PJ. GAGE: generally applicable gene set enrichment for pathway analysis. BMC Bioinformatics 2009;10(1):161.

(15) Luo W, Brouwer C. Pathview: an R/Bioconductor package for pathway-based data integration and visualization. Bioinformatics 2013;29(14):1830-1831.

(16) Truong D, Puleo J, Llave A, Mouneimne G, Kamm RD, Nikkhah M. Breast Cancer Cell Invasion into a Three Dimensional Tumor-Stroma Microenvironment. Scientific Reports 2016;6(1):34094.

(17) Beers J, Gulbranson DR, George N, Siniscalchi LI, Jones J, Thomson JA, et al. Passaging and colony expansion of human pluripotent stem cells by enzyme-free dissociation in chemically defined culture conditions. Nature Protocols 2012;7(11):2029-2040.

(18) Polo ML, Arnoni MV, Riggio M, Wargon V, Lanari C, Novaro V. Responsiveness to PI3K and MEK Inhibitors in Breast Cancer. Use of a 3D Culture System to Study Pathways Related to Hormone Independence in Mice. PLOS ONE 2010;5(5):e10786.

(19) Zhang Y, Lukacova V, Reindl K, Balaz S. Quantitative characterization of binding of small molecules to extracellular matrix. The Journal of Biochemical and Biophysical Methods 2006;67(2):107-122.

(20) Chen Y, Lan H, Wu Y, Yang W, Chiou A, Yang M. Epithelial-mesenchymal transition softens head and neck cancer cells to facilitate migration in 3D environments. Journal of Cellular and Molecular Medicine 2018;22(8):3837-3846.

(21) Hakkinen KM, Harunaga JS, Doyle AD, Yamada KM. Direct Comparisons of the Morphology, Migration, Cell Adhesions, and Actin Cytoskeleton of Fibroblasts in Four Different Three-Dimensional Extracellular Matrices. Tissue Engineering Part A 2011;17(5-6):713-724.

(22) Son H, Moon A. Epithelial-mesenchymal Transition and Cell Invasion. Toxicological research 2010;26(4):245-252.

(23) Kalluri R, Weinberg RA. The basics of epithelial-mesenchymal transition. Journal of Clinical Investigation 2009;119(6):1420-1428.

(24) Zhou P, Li B, Liu F, Zhang M, Wang Q, Liu Y, et al. The epithelial to mesenchymal transition (EMT) and cancer stem cells: implication for treatment resistance in pancreatic cancer. Molecular Cancer 2017;16(1):52.

(25) Ahmedah HT, Patterson LH, Shnyder SD, Sheldrake HM. RGD-Binding Integrins in Head and Neck Cancers. Cancers 2017;9(6):56.

(26) Wang K, Seo BR, Fischbach C, Gourdon D. Fibronectin Mechanobiology Regulates Tumorigenesis. Cellular and molecular bioengineering 2016;9:1-11.

(27) Simpson-Haidaris P, Rybarczyk B. Tumors and Fibrinogen. Annals of the New York Academy of Sciences 2001;936(1):406-425.

(28) Chen L, Xiao Z, Meng Y, Zhao Y, Han J, Su G, et al. The enhancement of cancer stem cell properties of MCF-7 cells in 3D collagen scaffolds for modeling of cancer and anti-cancer drugs. Biomaterials 2012;33(5):1437-1444.

(29) Hurst RE, Kyker KD, Bonner RB, Bowditch RD, Hemstreet,George P.,,3rd. Matrix-dependent plasticity of the malignant phenotype of bladder cancer cells. Anticancer Research 2003 Jul;23(4):3119-3128.

(30) Fliedner FP, Hansen AE, Jørgensen JT, Kjær A. The use of matrigel has no influence on tumor development or PET imaging in FaDu human head and neck cancer xenografts. BMC Medical Imaging 2016;16(1):5.

(31) Mouneimne G, Brugge JS. YB-1 Translational Control of Epithelial-Mesenchyme Transition. Cancer Cell 2009;15(5):357-359.

Figure legends:

Figure 1. SCC cell morphology observed under light microscope. Different shapes of UT-SCC-24B cells were observed depending on the used matrix. Cells on BSA gave similar morphology to the control. Cells were clustered on Matrigel, flat on fibronectin, and spindle on Myogel, fibrin, and collagen. Scale bar = 100 µm

Figure 2. SCC cell circularity. UT-SCC cells were cultured on different matrices and plastic (control) for 3 days and pictured on day 3 under light microscope. Cell circularity was measured using ImageJ software. In all cell lines represented in the figure, cells cultured on top of Matrigel showed the highest circularity value (above 0.8). Data are presented as means ± standard deviations.* $P \leq 0.05$. N=3.

Figure 3. SCC cell surface area. UT-SCC cells were cultured on different matrices and plastic (control) for 3 days and pictured on day 3 under light microscope. Cell surface area was measured using ImageJ software. UT-SCC-24B, UT-SCC-42A and UT-SCC-42B cells showed the highest cell surface area when cultured on Fibronectin, but this difference did not reach statistical significance. Data are presented as means ± standard deviations.* $P \leq 0.05$. N=3.

Figure 4. Matrices structure observed under scanning electron microscope. Coverslips were coated with different matrices and prepared for scanning electron microscope. Matrigel has a fiber sheet structure. Myogel's structure was in form of thin unorganized fibers together with

small globular proteins. As for fibrin, its fibers were thin. Collagen presented helical fibers structure. BSA and fibronectin did not show a fibril structure. Scale bar = 1 µm

Figure 5. SCC cells and matrix interaction observed under scanning electron microscope. UT-SCC 42B cells were cultured on coated coverslips with different matrices and prepared for scanning electron microscope. Cells cultured on BSA coated wells did not have any interaction with the matrix, similarly to the cells cultured on plastic. For Matrigel, cells formed small clusters on top of the matrix. Cells on fibronectin tend to be flat, more than any studied matrix, with a large surface area. As for Myogel, cells were gathered in groups and they were in contact with several fibers. In fibrin and collagen, cells were embedded within the matrix fibers. Scale bar = 10 µm

Figure 6. SCC cell proliferation rate on different matrices. UT-SCC cells were cultured on different matrices for three days and the cell proliferation rate was measured using luminescent cell viability assay. The proliferation rate for all the cell lines was the highest on fibrin and the lowest on collagen. This difference was significant for the fibrin-coated wells in case of UT-SCC-24A, 24B, and 42A cell lines and also for collagen in case of UT-SCC-24A and 42A cell lines. The red line represents the control value. Data are presented as means ± standard deviations.* P ≤ 0.05, ** ≤ 0.01, *** ≤ 0.001, **** ≤ 0.0001. N=3

Figure 7. SCC cell migration on different matrices. UT-SCC cells were cultured on different matrices and cell migration was evaluated using scratch wound cell migration assay. The migration rate was dependent on both the matrix and the cell line. Data are presented as migration curves and area under the curves as means ± standard deviations.* P ≤ 0.05, ** ≤ 0.01, *** ≤ 0.001, **** ≤ 0.0001. N=3.

Figure 8. SCC cells invasion through different matrices. UT-SCC cells were cultured on different matrices and cell invasion was evaluated using scratch wound cell invasion assay. The four studied cell lines showed the fastest invasion rate when cultured on Myogel-collagen and they did not invade through fibrin and Myogel-fibrin. Data are presented as invasion curves and area under the curves as means ± standard deviations.* ~~P~~ ≤ 0.05, ** ≤ 0.01, *** ≤ 0.001, **** ≤ 0.0001. N=3.

Figure 9. Spheroid invasion observed under light microscope. UT-SCC 42A cells were cultured in ultra-low attachment 96-well round bottom plate wells and embedded in different matrices. Spheroids were observed under light microscope. Scale bar = 100 µm.

Figure 10. SCC spheroid invasion though different matrices. UT-SCC cells were cultured in ultra-low attachment 96-well round bottom plate wells and embedded in different matrices. For UT-SCC-24A, 42A, and 42B, Myogel-fibrin matrix showed the fastest spheroids invasion, followed by Myogel-collagen. For UT-SCC-24B cells invaded faster in Myogel-collagen followed by Myogel-fibrin. Data are presented as invasion curves and area under the curves as means ± standard

deviations. *≤0.05, *** ≤ 0.001, **** ≤ 0.0001. N=3.

List of Supporting Information:

Supplementary Table 1. HNSCC cell lines details. Clinical and pathological characteristics of the HNSCC cell lines. TNM is based on

Supplementary Table 2. Number of differentially expressed genes of UT-SCC-24A and B cultured on different matrices. Results of mRNA microarray showing the number of differentially expressed genes between cells cultured on plastic and cells cultured on matrices. The genes that passed the filter criteria had a $p<0.05$ and a fold change ≤-2 or ≥2. Transcriptome analysis console software was used to analyze the data

Supplementary Table 3. The most affected genes of UT-SCC cells cultured on different matrices. Results of mRNA microarray showing the most significantly affected genes (up- down-regulated)

by each matrix we used. The genes that passed the filter criteria had a $p<0.05$ and a fold change ≤-2 or ≥2. Transcriptome analysis console software was used to analyze the data.

Supplementary Table 4. Number of differentially expressed pathways of UT-SCC-24A and B cultured on different matrices. Results of the gene set enrichment analysis (GSEA) showing the number of the differentially represented pathways between cells cultured on plastic and cells cultured on matrices. The pathways that passed the filter criteria had a $p<0.05$.

Supplementary Table 5. The 10 most affected pathways of UT-SCC cells cultured on different matrices. Results of the gene set enrichment analysis (GSEA) showing the 10 most differentially expressed pathways between cells cultured on plastic and cells cultured on matrices. The pathways that passed the filter criteria had a $p<0.05$.

Supplementary video 1: migration of the UT-SCC-42A cells on top of Myogel.

Supplementary video 2: the invasion of the UT-SCC-42A within Myogel-collagen.

Figure 1
Click here to download high resolution image

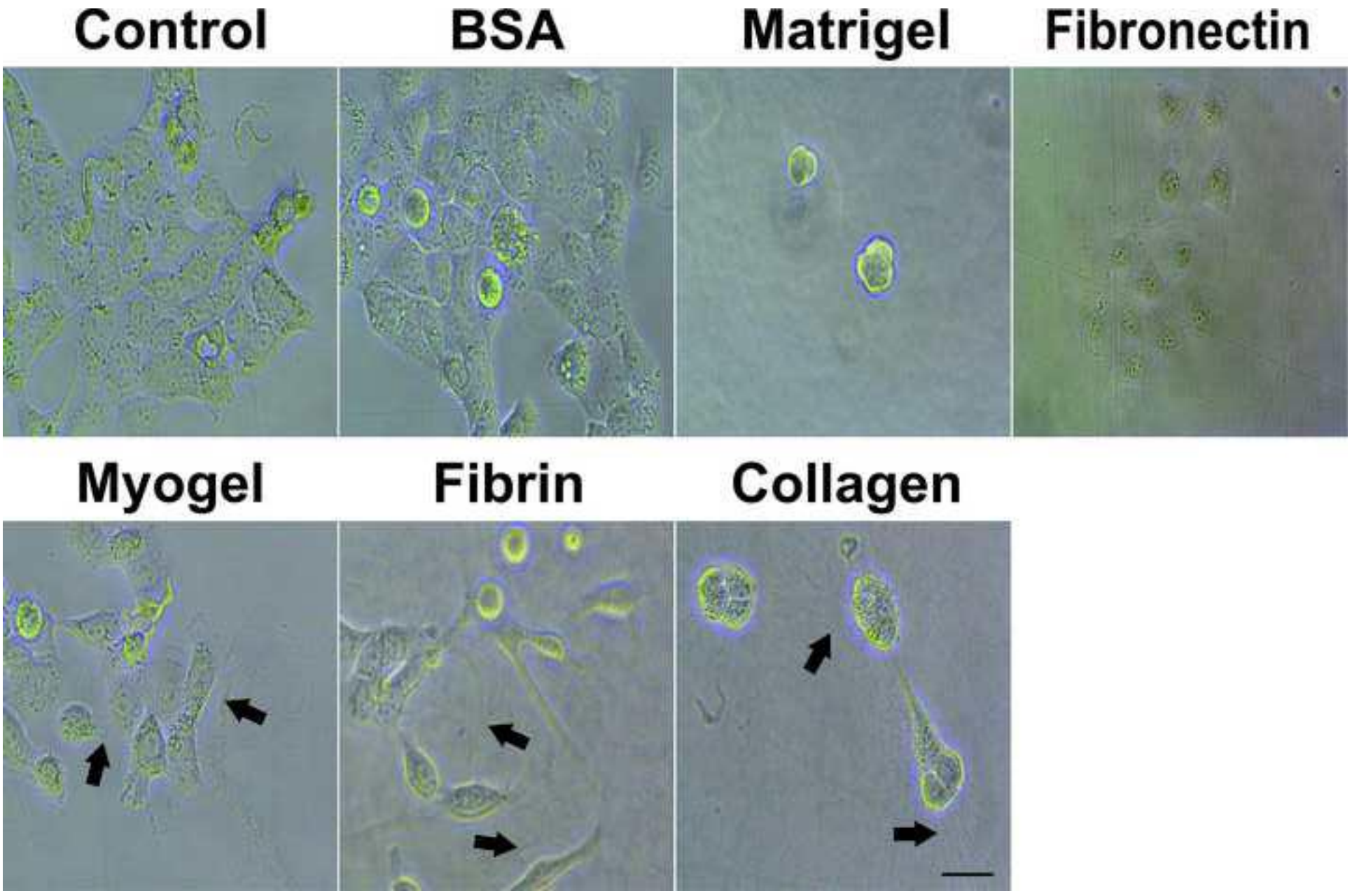

Figure 2
Click here to download high resolution image

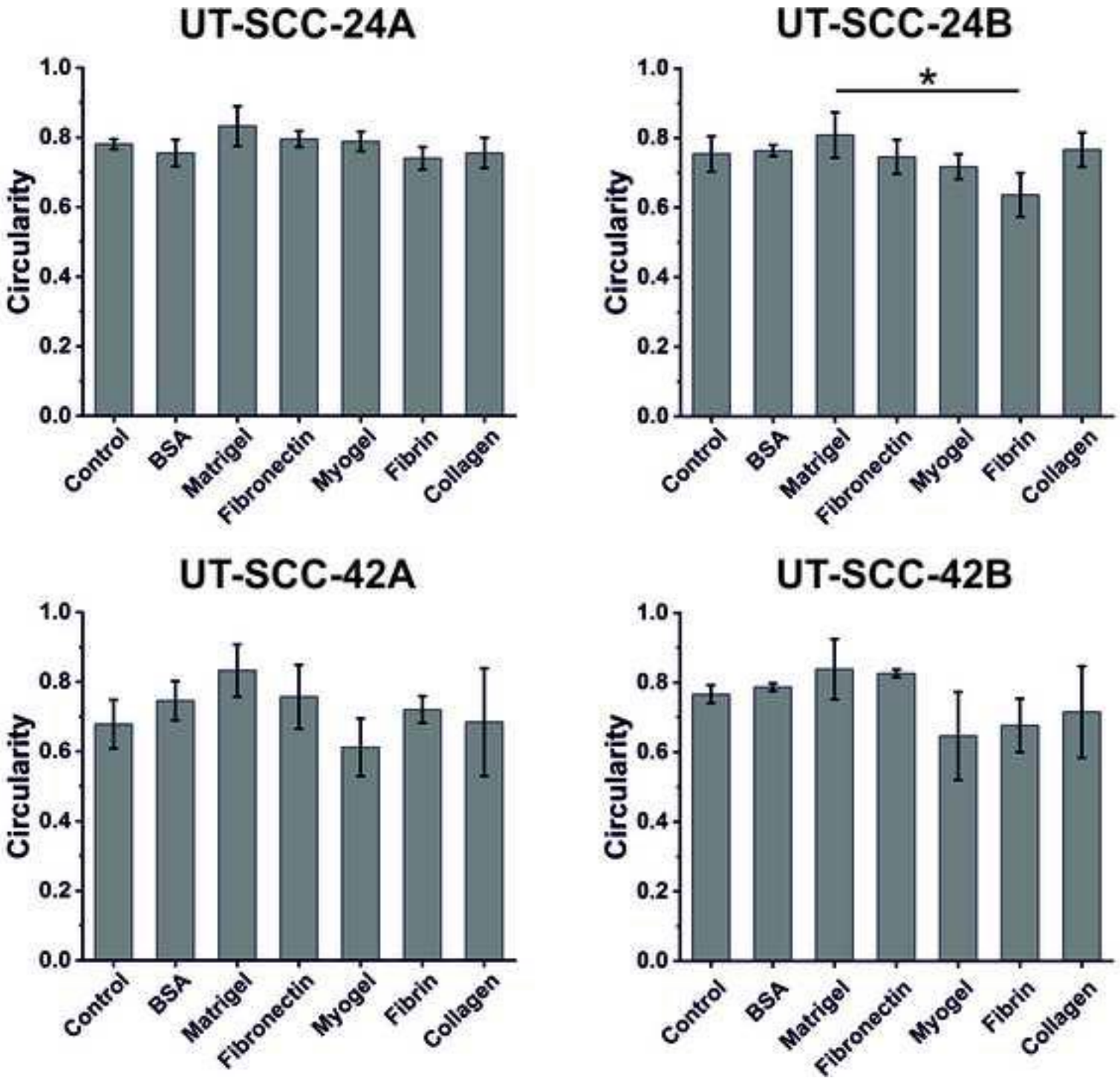

Figure 3
Click here to download high resolution image

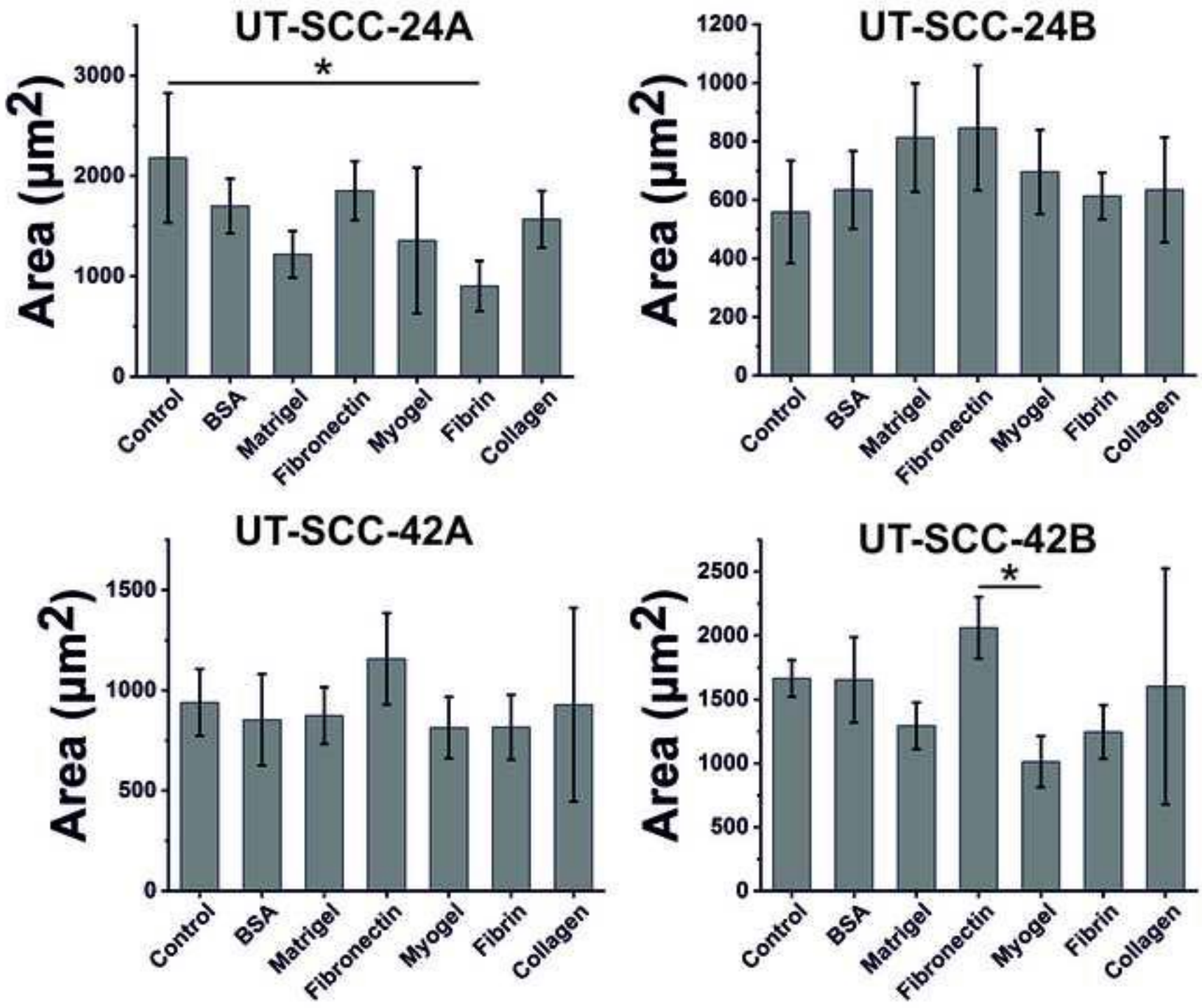

Figure 4
Click here to download high resolution image

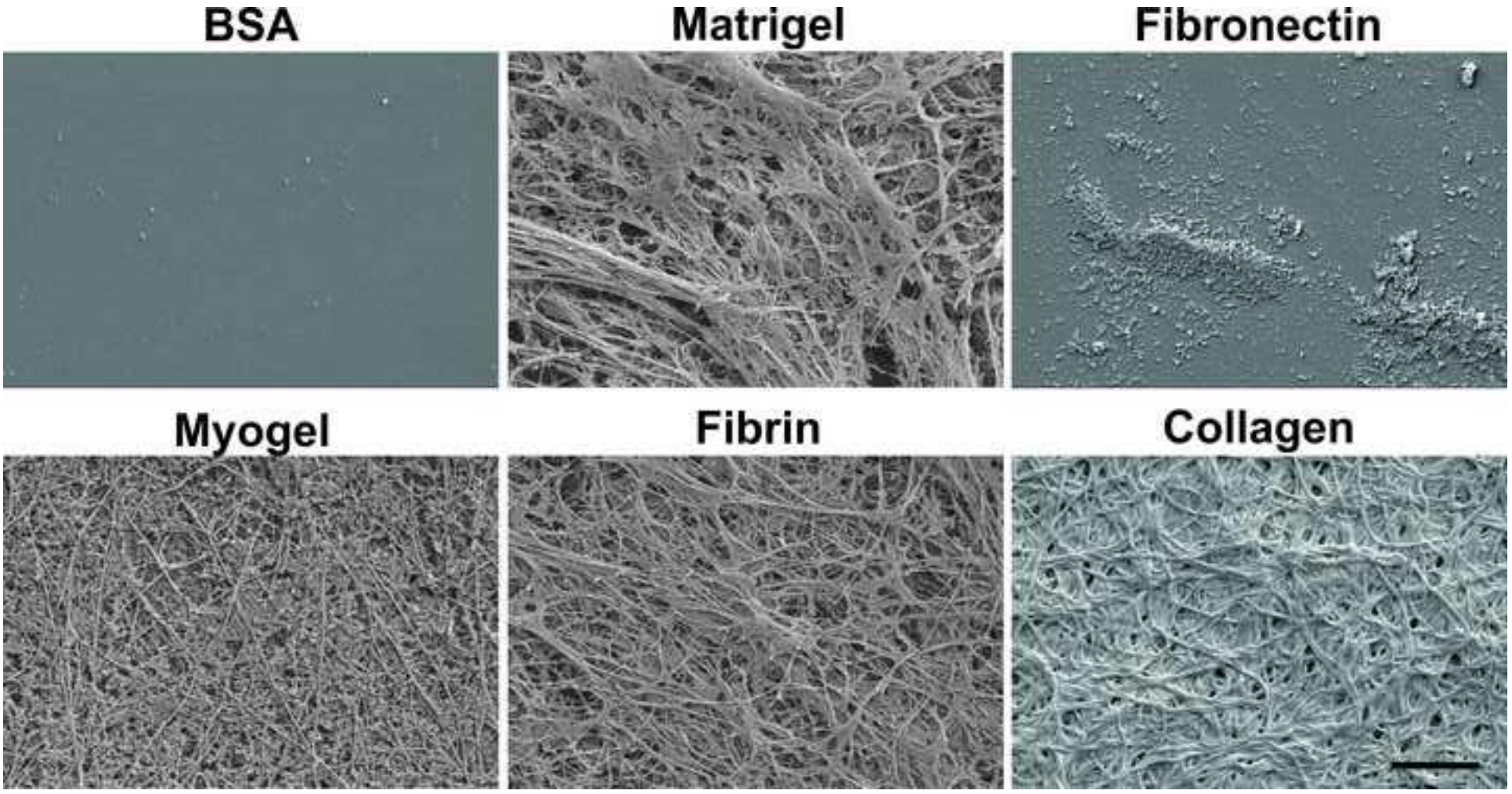

Figure 5
Click here to download high resolution image

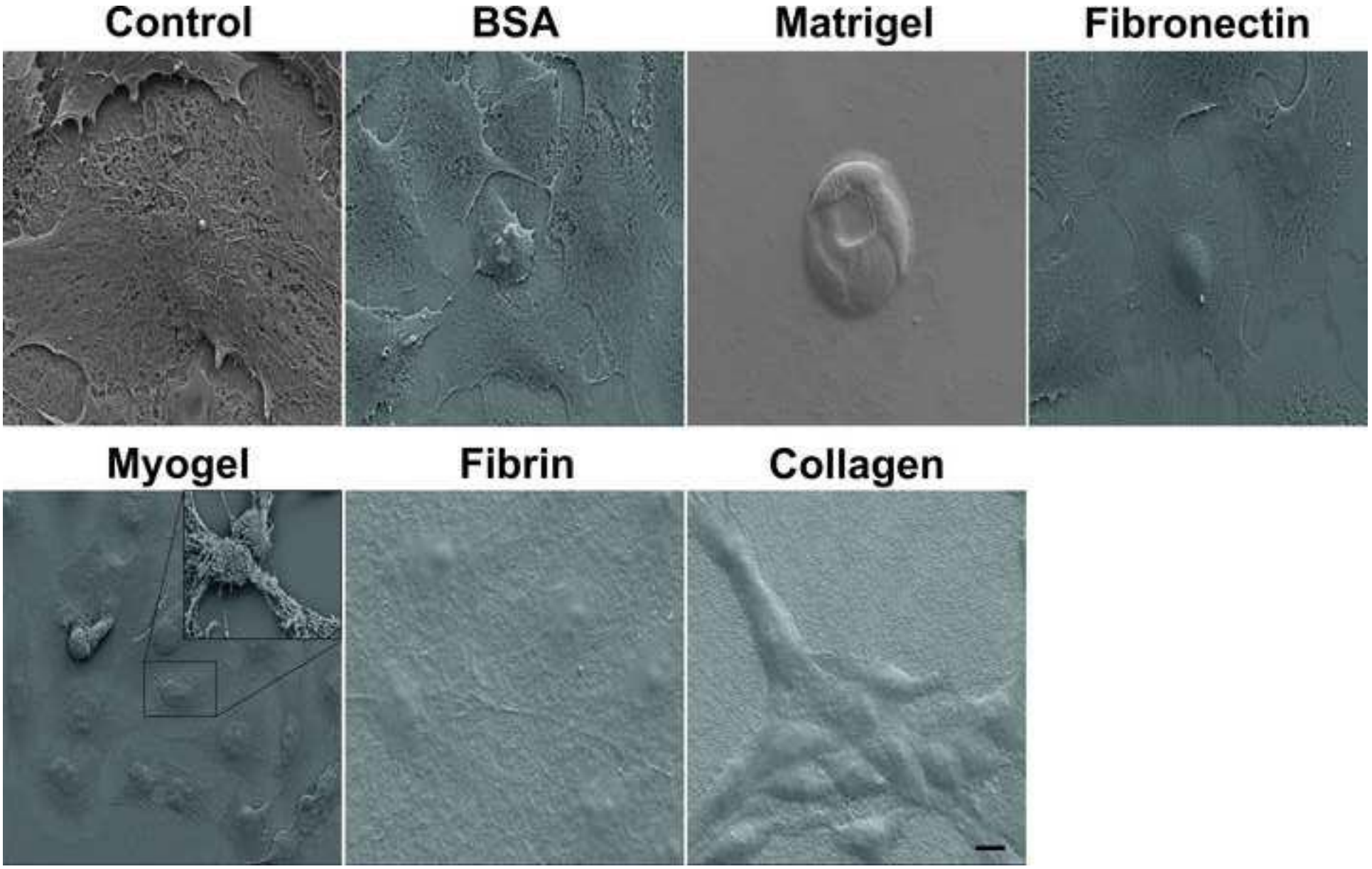

Figure 6
Click here to download high resolution image

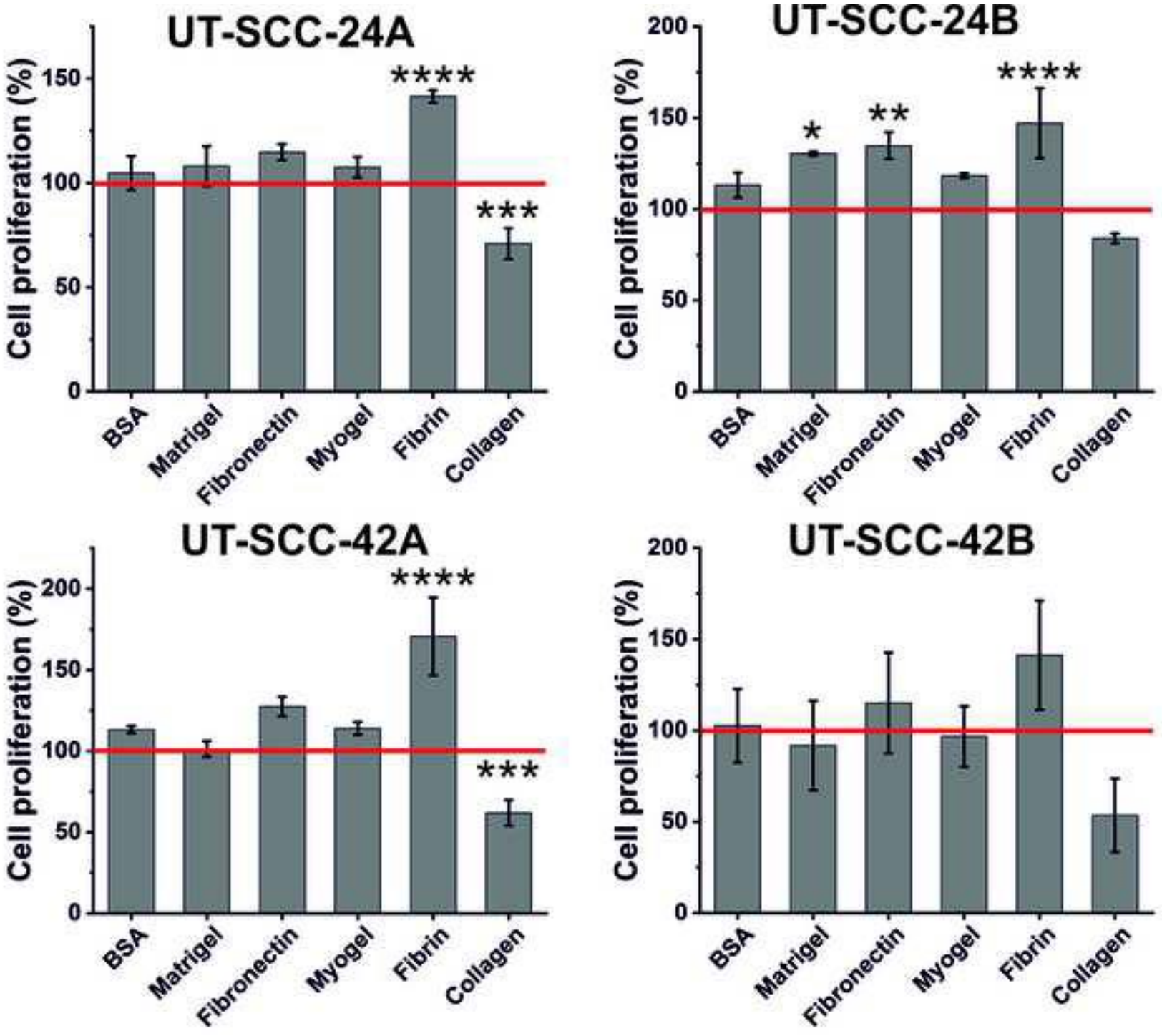

Figure 7
Click here to download high resolution image

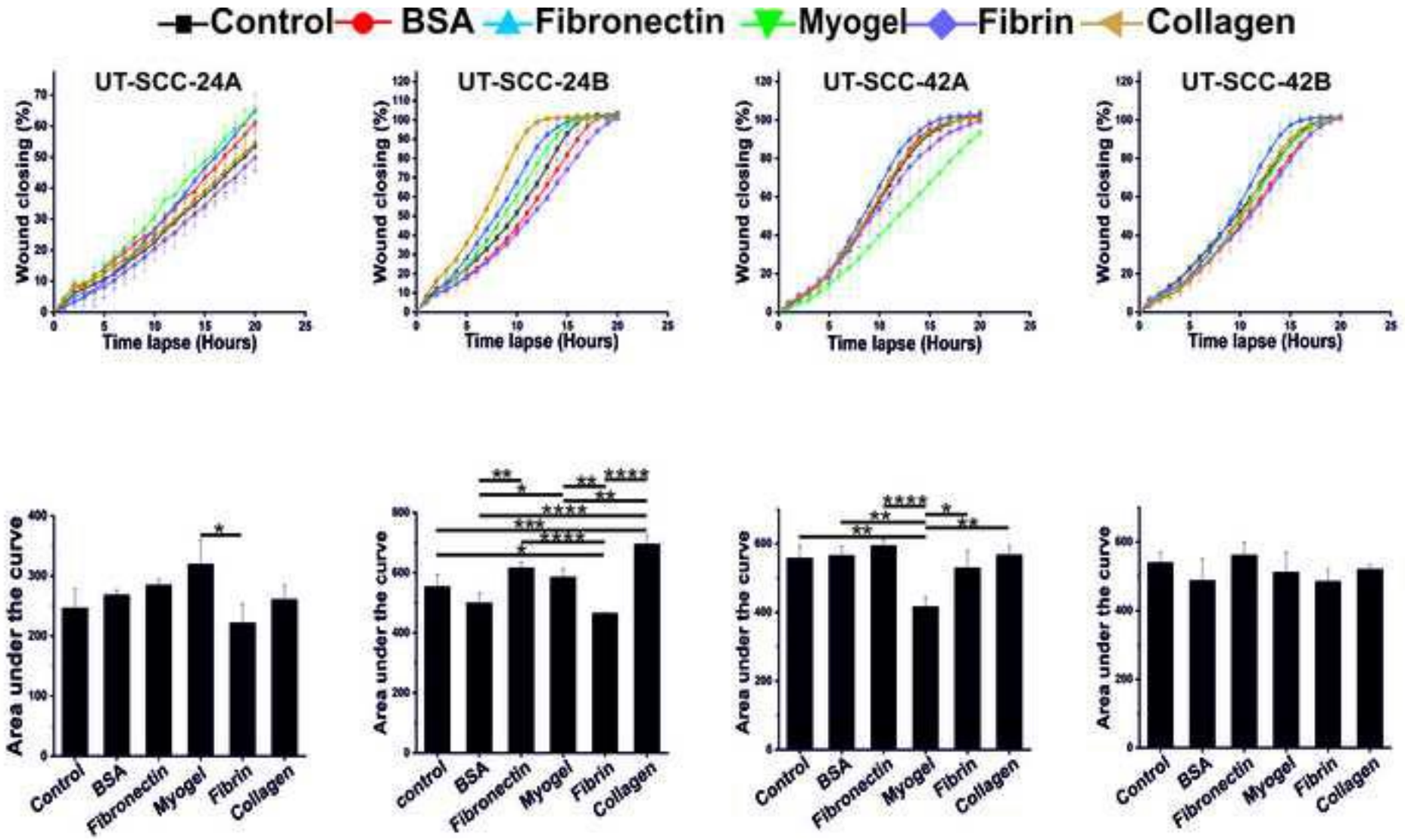

Figure 8
Click here to download high resolution image

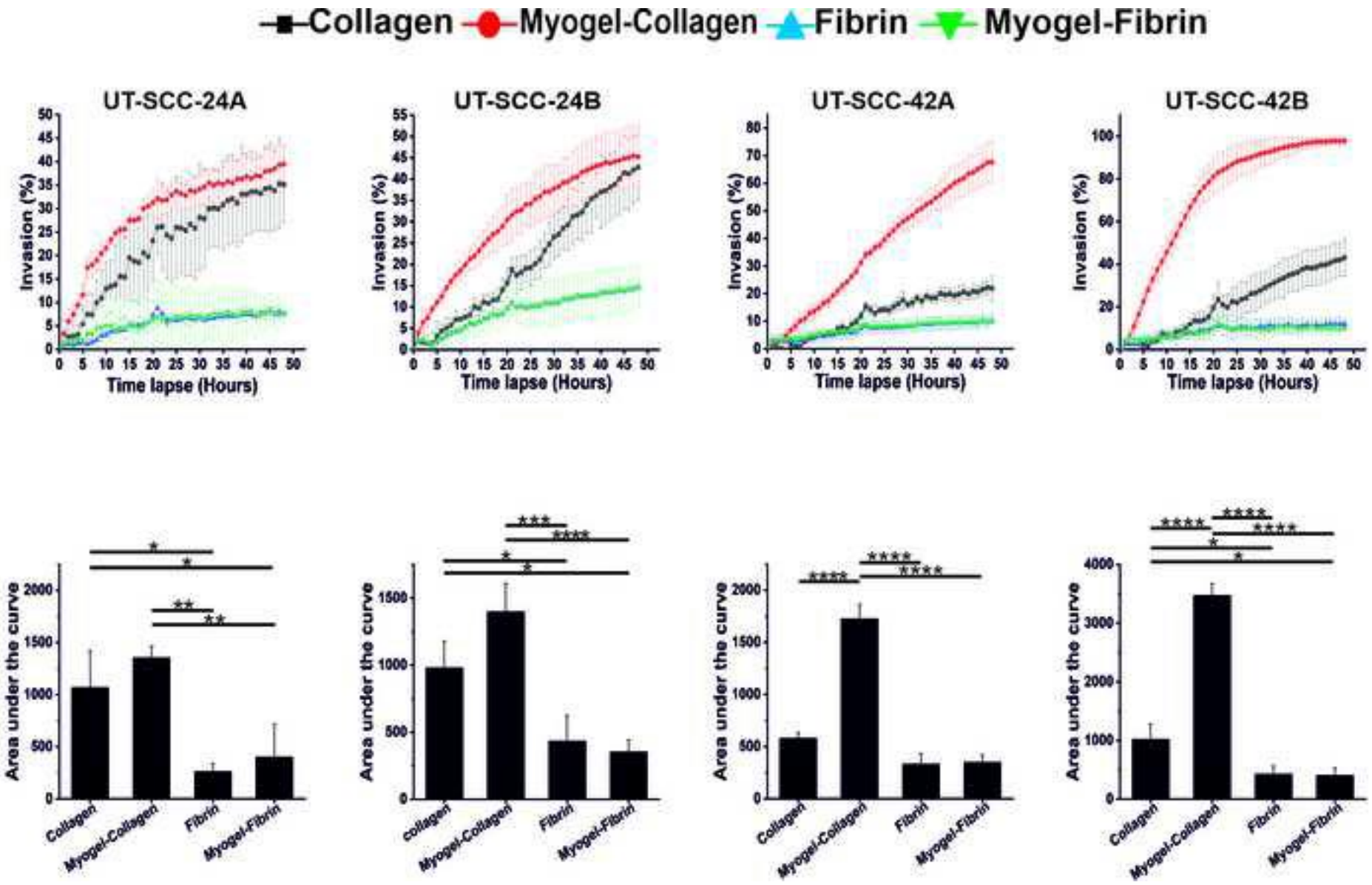

Figure 9
Click here to download high resolution image

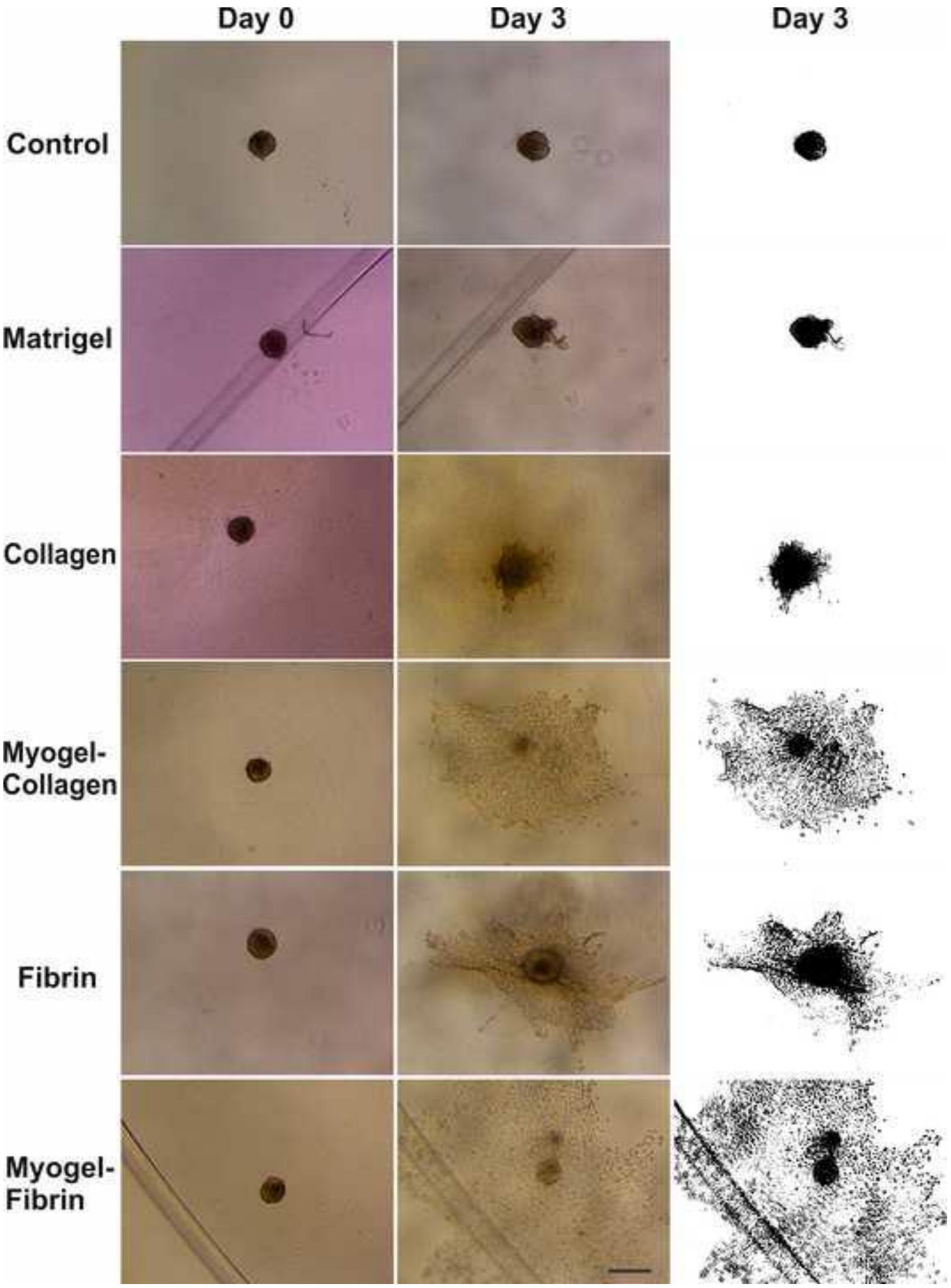

Figure10
Click here to download high resolution image

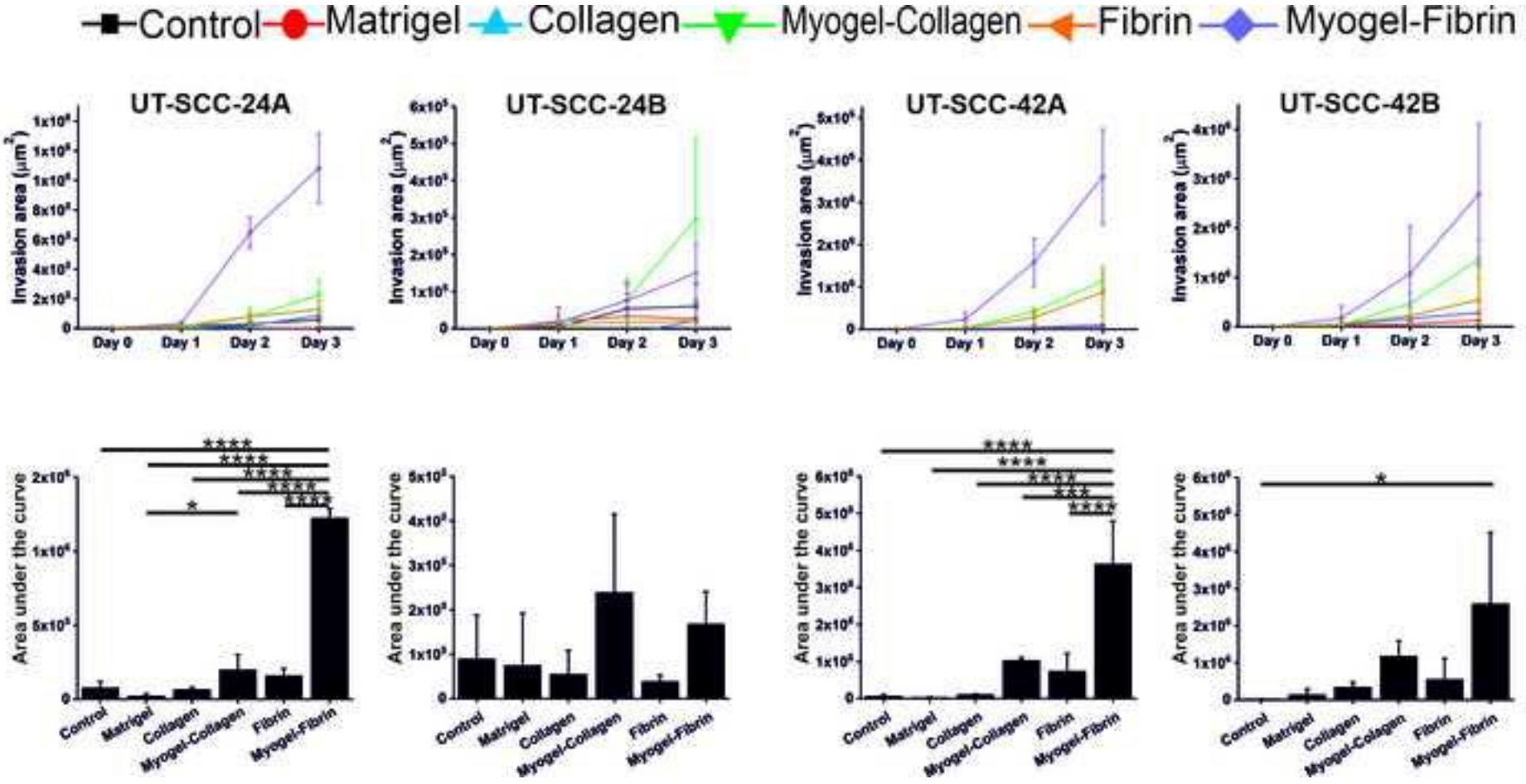

Video 1

Click here to download Supplementary material for online publication only: Supplement Video 1.mp4

Video 2

Click here to download Supplementary material for online publication only: Supplement Video 2.mp4

Supplementary material for online publication only
Click here to download Supplementary material for online publication only: Table 1.docx

Supplementary material for online publication only
Click here to download Supplementary material for online publication only: Table 2.docx

Supplementary material for online publication only
Click here to download Supplementary material for online publication only: Table 3.docx

Supplementary material for online publication only
Click here to download Supplementary material for online publication only: Table 4.docx

Supplementary material for online publication only
Click here to download Supplementary material for online publication only: Table 5.docx

Authors´ contributions:

Wafa Wahbi: Conceptualization, Methodology, Validation , Formal analysis , Software, Investigation , Data Curation, Writing - Original Draft , Writing - Review & Editing , Visualization , Project administration.

Ahmed Al-Samadi: Conceptualization, Methodology, Validation, Formal analysis, Software, Investigation, Data Curation, Writing - Review & Editing, Visualization, Project administration, Supervision.

Tuula Salo: Conceptualization, Methodology, Supervision, Writing - Review & Editing.

Reidar Grenman: Conceptualization, Methodology, Writing - Review & Editing.

Erika Naakka: Conceptualization, Data Curation, Formal analysis, Writing - Review & Editing

Katja Tuomainen: Conceptualization, Data Curation, Formal analysis, Writing - Review & Editing.

Ilida Suleymanova: Software, Writing - Review & Editing.

Annamari Arpalahti: Data Curation, Writing - Review & Editing.

Ilkka Miinalainen: Data Curation, Writing - Review & Editing.

Juho Vaananen: Formal analysis, Writing - Review & Editing.

Outi Monni: Methodology, Writing - Review & Editing.

***Conflict of Interest Form**

Declaration of interests

☒ The authors declare that they have no known competing financial interests or personal relationships that could have appeared to influence the work reported in this paper.
☐The authors declare the following financial interests/personal relationships which may be considered as potential competing interests:
